



# Rolling Resistance Validation

Minnesota  
Department of  
Transportation

**RESEARCH  
SERVICES  
&  
LIBRARY**

**Office of  
Transportation  
System  
Management**

Germana Paterlini, Principal Investigator  
FuelMiner, Inc.

**July 2015**

Research Project  
Final Report 2015-39



To request this document in an alternative format call [651-366-4718](tel:651-366-4718) or [1-800-657-3774](tel:1-800-657-3774) (Greater Minnesota) or email your request to [ADArequest.dot@state.mn.us](mailto:ADArequest.dot@state.mn.us). Please request at least one week in advance.

## Technical Report Documentation Page

1. Report No. MN/RC 2015-39	2.	3. Recipients Accession No.	
4. Title and Subtitle Rolling Resistance Validation		5. Report Date July 2015	
		6.	
7. Author(s) Germana Paterlini, Sermet Yucel, Melinda Moran Lucking, Jon Magnuson		8. Performing Organization Report No.	
9. Performing Organization Name and Address FuelMiner, Inc. 3601 Minnesota Drive, Suite 690 Minneapolis, MN 55435		10. Project/Task/Work Unit No.	
		11. Contract (C) or Grant (G) No.	
12. Sponsoring Organization Name and Address Minnesota Department of Transportation Research Services & Library 395 John Ireland Boulevard, MS 330 St. Paul, Minnesota 55155-1899		13. Type of Report and Period Covered Final Report	
		14. Sponsoring Agency Code	
15. Supplementary Notes <a href="http://www.lrrb.org/pdf/201539.pdf">http://www.lrrb.org/pdf/201539.pdf</a>			
16. Abstract (Limit: 250 words)  <p>The rolling resistance, contact forces and fuel consumption of a heavy duty truck were computed as a function of pavement type. Measurements were conducted at the Mainline MnROAD test track near Albertville, Minnesota and at two highway sections with distressed pavements. Test procedure consisted of driving the instrumented MnROAD heavy-duty truck on the selected pavement sections while recording signals from the chassis-mounted accelerometers, differential GPS, and the Controller Area Network. The truck was driven at cruise speeds of 55 and 64 MPH on roads with live traffic and at cruise speeds from 30 to 65 MPH on the Mainline. In addition, weather data from two MnROAD stations, wind velocity from two ultrasonic anemometers, road elevation, and IRI were collected during the tests. Data were analyzed with a novel and comprehensive mechanistic model of vehicle dynamics. Dynamical rolling resistance and its contribution to fuel consumption was estimated from the spectra analysis of accelerometers signals. The coefficient of rolling resistance of the truck tires varied from 0.0044 to 0.0072 on the Mainline cells. Fuel consumed by the rolling resistance force at 30 MPH varied between 0.006 liter and 0.009 liter per cell, for an average consumption of 5 liter/100 km. Rolling resistance was 0.0072 on bituminous TH 66 and 0.0061 on concrete TH 10 sections. Spectral analysis of accelerometer data revealed vibrational modes unique to either bituminous or concrete pavements. The power loss caused by the vibrations of suspensions and tires was also computed.</p>			
17. Document Analysis/Descriptors Rolling resistance, Dynamics, Vehicle dynamics, Motor vehicle dynamics, Heavy duty vehicles, Accelerometers, Roughness, Fuel consumption, Fuel processing, ECU, CAN bus		18. Availability Statement No restrictions. Document available from: National Technical Information Services, Alexandria, Virginia 22312	
19. Security Class (this report) Unclassified	20. Security Class (this page) Unclassified	21. No. of Pages 44	22. Price

# **Rolling Resistance Validation**

## **Final Report**

*Prepared by:*

Germana Paterlini  
Sermet Yucel  
Melinda Moran Lucking  
Jon Magnuson  
FuelMiner, Inc.

**July 2015**

*Published by:*

Minnesota Department of Transportation  
Research Services & Library  
395 John Ireland Boulevard, MS 330  
St. Paul, Minnesota 55155-1899

This report represents the results of research conducted by the authors and does not necessarily represent the views or policies of the Minnesota Department of Transportation and/or FuelMiner Inc. This report does not contain a standard or specified technique.

The authors and the Minnesota Department of Transportation and/or FuelMiner, Inc. do not endorse products or manufacturers. Trade or manufacturers' names appear herein solely because they are considered essential to this report.

## **ACKNOWLEDGMENTS**

The authors would like to thank Mr. David Van Deusen of MnDOT's Office of Materials and Road Research for his support of this project, assisting in the selection of road sections and performing International Roughness Index (IRI) measurements; and Ms. Maureen Jensen, for providing funding with MnDOT for this project. The authors wish to express their gratitude to Mr. Ben Worel and his excellent staff for providing logistics support and measurements at the Albertville, Minnesota, facility and offsite. In particular, the authors would like to thank Mr. Doug Lindenfelser for expertly driving the MnROAD truck, Mr. Robert Strommen for providing weather data and assistance with the truck instrumentation, and Mr. Jack Hendon for elevation measurements at the Albertville facility.

# TABLE OF CONTENTS

Chapter 1: Introduction .....	1
Chapter 2: Theoretical and computational approach .....	3
2.1 Estimation of Contact and Rolling Resistance Forces .....	3
2.2 Estimation of Fuel Consumption Breakdown .....	5
2.3 Estimation of Power Consumed by Dynamic Rolling Resistance .....	6
2.4 Spectral Analysis of Vibrations from Tires and Suspensions .....	7
Chapter 3: Numerical considerations .....	8
Chapter 4: Experimental setup .....	10
4.1 Vehicle Instrumentation .....	10
4.2 Test Procedure .....	11
4.3 Data Collection and Format .....	12
Chapter 5: Test Pavements .....	13
5.1 MnROAD Mainline .....	13
5.1.1 Mainline – Road Elevation and Grade .....	14
5.1.2 Mainline – IRI .....	14
5.1.3 Mainline – Environmental Conditions .....	15
5.2 TH 10 – Concrete Pavement .....	15
5.2.1 Road Elevation and Grade .....	15
5.2.2 TH 10 – IRI .....	15
5.2.3 TH 10 – Environmental Conditions .....	16
5.3 TH 66 – Bituminous Pavement .....	18
5.3.1 TH 66 – Road Elevation and Grade .....	18
5.3.2 TH 66 – IRI .....	18
5.3.3 TH 66 – Environmental Conditions .....	18
Chapter 6: Data analysis .....	20
6.1 Contact Forces .....	20
6.2 Rolling Resistance and Fuel Consumption .....	21
6.2.1 Coefficient of Rolling Resistance of Mainline Cells .....	21
6.2.2 Rolling Resistance of TH 10 and TH 66 .....	22
6.2.3 Fuel Consumption of Mainline Cells .....	24
6.2.4 Estimated Fuel Consumption Breakdown .....	24

6.3 Spectral Analysis and Power Loss from Suspensions and Tires .....	26
6.3.1 Mainline .....	26
6.3.2 TH 10 and TH 66 .....	28
6.4 Contributions of Suspensions and Tires to Annual Fuel Consumption .....	30
Chapter 7: Conclusions .....	31
Chapter 8: References .....	33

## LIST OF FIGURES

Figure 2.1 Quarter Car Model (QCM).....	3
Figure 2.2 Estimated fuel consumption breakdown of the MnROAD truck traveling on the Mainline at 64 MPH.....	5
Figure 4.1 Instrumentation of MnROAD Truck, driver side view (revised from Ref. [12]).....	10
Figure 4.2 FuelMiner Logger.....	11
Figure 4.3 Ultrasonic anemometer near TH 10. ....	12
Figure 5.1 Schematic of MnROAD pavement cells. ....	13
Figure 5.2 Mainline road grade. Cell numbers are shown at the bottom of the graph. ....	14
Figure 5.3 IRI of MnROAD Mainline (westbound direction).....	14
Figure 5.4 TH 10 – Concrete pavement road section. ....	16
Figure 5.5 TH 10 – Elevation. ....	17
Figure 5.6 TH 10 – Road grade. ....	17
Figure 5.7 TH 10 – IRI. ....	17
Figure 5.8 TH 66 – Bituminous pavement road section. ....	19
Figure 5.9 TH 66 Road grade ....	19
Figure 5.10 TH 66 – IRI. ....	19
Figure 6.1 Mainline – Contact forces. ....	20
Figure 6.2 Coefficient of rolling resistance computed from data recorded at 30 MPH and at 64 MPH. Blue: 30 MPH; red: June 12; green: June 13. ....	22
Figure 6.3 Fuel consumed by Rolling Resistance per cell.....	24
Figure 6.4 Estimated fuel breakdown at 30 MPH and 64 MPH on the Mainline.....	25
Figure 6.5 Estimated fuel breakdown at 55 MPH on TH 10 and TH 66. ....	25
Figure 6.6 Vibrational modes computed from accelerometer TLR2 on the Mainline.....	26
Figure 6.7 Vibrational modes computed from accelerometer TLF2 on the Mainline. ....	27
Figure 6.8 Vibrational modes computed from accelerometer TLF1 on the Mainline. ....	27
Figure 6.9 Power loss at 30MPH for eastbound and westbound directions on Mainline. ....	28
Figure 6.10 Vibrational modes observed on TH 10. Spectra are overlaid with a shift of 30 g <sup>2</sup> /Hz. ....	29
Figure 6.11 Vibrational modes observed on TH 66. Spectra are overlaid with a shift of 30 g <sup>2</sup> /Hz. ....	29

## LIST OF TABLES

Table 2.1 Notation. ....	4
Table 3.1 Computed Physical Quantities.....	9
Table 5.1 Length of Mainline concrete panels.....	13
Table 5.2 Mainline environmental conditions. ....	15
Table 5.3 TH 10-GPS Coordinates. ....	16
Table 5.4 TH 10 Environmental conditions.....	16
Table 5.5 TH 66 – GPS Coordinates. ....	18
Table 5.6 TH 66 – Environmental conditions.....	18
Table 6.1 Total, sprung and unsprung mass of MnROAD truck. ....	20
Table 6.2 Vehicle mass. ....	21
Table 6.3 CRR of Mainline Cells (30 MPH) ....	23

Table 6.4 CRR of TH 10 and TH 66.....	23
Table 6.5 Average power loss of bituminous and concrete sections of Mainline. ....	28
Table 6.6 Power loss from tires and suspensions on TH 66 and TH 10 .....	30

## EXECUTIVE SUMMARY

The Minnesota Department of Transportation contracted with FuelMiner Inc. of Minneapolis, Minnesota, to measure rolling resistance, contact forces and fuel consumption due to the interaction of a heavy duty vehicle with asphalt and concrete pavements. Measurements were obtained at the Mainline MnROAD test track near Albertville, Minnesota, and at two highway sections with distressed pavements. These segments were a two-mile segment of TH 66 near Good Thunder, Minnesota, and a five-mile section of TH 10 near Sartell, Minnesota. Tests were conducted over several days from April to October 2014. Test procedure consisted of driving the instrumented MnROAD heavy-duty truck on the selected pavement sections while recording signals from the chassis-mounted accelerometers, differential GPS, and the Controller Area Network. The truck was driven at cruise speeds of 55 and 64 MPH on roads with live traffic and at cruise speeds from 30 to 65 MPH on the Mainline. In addition, weather data from two MnROAD stations, wind velocity from two ultrasonic anemometers, road elevation, and International Roughness Index (IRI) were collected during the tests. Data were analyzed with a novel and comprehensive mechanistic model of vehicle dynamics. Dynamical rolling resistance and its contribution to fuel consumption were estimated from the spectra analysis of accelerometers signals. Based on the data collected, the analysis provided the following results. The coefficient of rolling resistance of the truck tires varied from 0.0044 to 0.0072 on the Mainline cells. Fuel consumed by the rolling resistance force at 30 MPH varied between 0.006 liter and 0.009 liter per cell, for an average consumption of 5 liter/100 km. Rolling resistance was 0.0072 on bituminous TH 66 and 0.0061 on concrete TH 10, for a vehicle speed of 55 MPH. Spectral analysis of accelerometer data was performed to examine how different pavement types contribute to dynamic rolling resistance. The spectral analysis revealed vibrational modes unique to either bituminous or concrete pavements. In particular, joints between concrete panels gave rise to vibrations at 2.9 Hz corresponding to panel length of 15' on the Mainline or 27' on TH 10. The fuel consumption component attributed to dynamic rolling resistance was computed to be 0.3 liter/100 km higher on the TH 10 section compared to the TH 66 section.

## CHAPTER 1: INTRODUCTION

The load of vehicles traveling on roads stresses the pavement's surface, and vice versa, pavement conditions affect vehicle performance and wear. Surface roughness creates longitudinal frictional forces between tires and pavement, whereas surface unevenness causes the vehicle to bounce vertically thereby exciting the suspensions. Together, these mechanisms define the pavement-specific rolling resistance. Fuel is consumed to overcome rolling resistance and accelerate or sustain vehicle's motion. Therefore, understanding the sources of pavement-related rolling resistance can lead to cost effective pavement design and maintenance, increased safety and comfort, and lower operating costs.

The contribution of rolling resistance to fuel consumption is greater for heavy duty trucks than passenger cars because of their heavy loads and diverse axle configurations. In 2012, US heavy trucks consumed 44 billion gallons of diesel fuel [1], of which, four to seven billion were spent overcoming rolling resistance. Even a few percent decrease in rolling resistance can save millions of gallons of fuel a year. Fuel is also the largest operating cost for truck fleets, at par or greater with drivers' salary [2].

Several approaches have been proposed to estimate vehicle operating costs [3]. Empirical models do not make assumptions on the nature of pavement-vehicle interaction but build the system's parameters from correlations in the data [3]. The model developed by the World Bank (Highway Development and Management Model, HDM-3 and HDM-4) is a mechanistic-empirical hybrid model [3]. Its foundation is a physical model of vehicle-pavement interaction, but its calibration process can be cumbersome because experimental data are fitted to a large number of adjustable parameters and formulas [3]. Application of HDM-4 fuel consumption model to heavy trucks underestimated fuel consumption and showed dependency on cruise control engagement [3]. Mechanistic models, on the contrary, are based on physics of vehicle dynamics [3]. They entail fewer parameters than hybrid models, but they can be difficult to simulate, and can lead to systematic errors if the physical model is incomplete or inaccurate.

FuelMiner has developed a fully mechanistic model of vehicle operating costs, and a method for time-resolved analysis of tractive and resistive forces acting on the vehicle, including aerodynamic drag, road grade, and rolling resistance. The approach, referred to as TRMA-VOC (Time-Resolved Mechanistic Analysis of Vehicle Operating Costs, hereafter "TRMA"), has been validated experimentally [4]. TRMA makes use of on-road truck data and a handful of known variables (such as vehicle mass) in a Kalman Filter to minimize the random errors and optimally estimate model parameters. The time-resolved analysis provides two major benefits: first, it isolates the rolling resistance contribution from other resistive forces, such as aerodynamic drag; second, it can compute the fuel distribution for trip segments as short as one second, or about 10 feet for a truck traveling at 60 MPH [4].

The goal of this project was to measure fuel consumption by a heavy duty truck and, with TRMA, isolate the fuel consumptions due to numerous forces acting on the vehicle, including longitudinal forces of pavement-vehicle interaction.

FuelMiner first validated TRMA with truck data previously collected at the MnROAD research facility in Albertville, Minnesota [4]. In these experiments, the rolling resistance was estimated for the entire 3.5 miles Mainline MnROAD section, and it did not explicitly compute dynamic rolling resistance. In this project, TRMA was applied to the analysis of the each pavement type at the MnROAD facility and two highway segments with distressed bituminous and concrete pavement, respectively. The contribution of suspensions and tires to dynamic rolling resistance was computed directly from the spectral analysis of accelerometers instrumented on the heavy vehicle.

This final report presents the results of the TRMA to estimate the following:

- Coefficient of Rolling Resistance (CRR) as a function of each pavement type at State's MnROAD facility
- Contact Forces as a function of each pavement type at State's MnROAD facility
- Fuel consumption as a function of each pavement type at State's MnROAD facility

The experimental and analytical approach in this report describes the “vehicle plus pavement point of view” of pavement-vehicle interactions. As such, it complements existing methods employed by civil engineers to study rolling resistance and fuel consumption by tire-pavement interaction. The reports highlights the benefits of the TRMA and suggests improvements in the experimental setup for further refinement of the dynamical models and numerical analysis of data.

## CHAPTER 2: THEORETICAL AND COMPUTATIONAL APPROACH

### Estimation of Contact and Rolling Resistance Forces

TRMA has been described in detail by Yucel et al [4]. The vehicle dynamics is a modified Quarter Car Model (QCM, Figure 2.1), that explicitly takes into account the coupling between the motion of tires and suspensions in the direction of travel and perpendicular to the ground [4]. The vehicle dynamics equation include, in addition to QCM, road grade, aerodynamics drag, driveline friction, the tractive force of the engine, and dissipative forces from engine friction and accessories. Non-linear Kalman Filter is ideal for analyzing noisy time series, such as those reported here. TRMA utilizes it to estimate states and parameters from the recorded time series of vehicle and environment data.

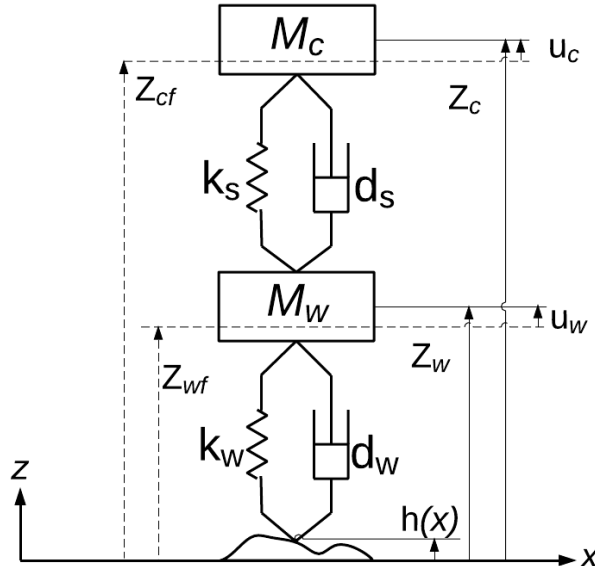


Figure 2.1 Quarter Car Model (QCM).

According to QCM, the ground contact force  $F_z$  acting on the tire is [4]:

$$F_z = (M_w + M_c)g \cos(\chi_{road}) + M_w \ddot{u}_w + M_c \ddot{u}_c \quad (2.1)$$

The notation is described in Table 2.1.

The force  $F_z$  on the ground is the normal component of the gravitational force and the forces generated by the axle and suspension vibrations. We assume that dynamical rolling resistance is accounted by the normal force variations. The rolling resistance is then given by [4]:

$$F_{RR} = -\mu_{RR} F_z \quad (2.2)$$

In Equation 2.2,  $\mu_{RR}$  is the Coefficient of Rolling Resistance (CRR) of a tire on a flat and rigid surface.

**Table 2.1 Notation.**

$d_s$	Suspension viscous damping constant
$d_w$	Tire viscous damping constant
$F_{RR}$	x component of the rolling resistance force
$F_z$	z component of the force exerted on the tire by the ground
$g$	Gravitational acceleration on the surface of earth
$h(x)$	Ground height from a vertical reference height.
$k_s$	Suspension spring constant
$k_w$	Tire spring constant
$M_c$	Sprung mass
$M_w$	Unsprung mass
$u_c$	$z_c - z_{cf}$
$u_{c0}$	$z_{c0} - z_{cf}$
$u_w$	$z_w - z_{wf}$
$u_{w0}$	$z_{w0} - z_{wf}$
$x$	Coordinate axis parallel to the surface of the earth and in the direction of vehicle travel
$z$	Vertical coordinate axis perpendicular and away from to the surface of the earth
$z_c$	Sprung mass vertical location
$z_{cf}$	Sprung mass location when sprung and unsprung mass is zero
$z_w$	Unsprung mass vertical location
$z_{wf}$	Unsprung mass location when sprung and unsprung mass is zero
$\mu_{RR}$	Rolling resistance force coefficient
$\chi_{road}$	Road slope angle

## Estimation of Fuel Consumption Breakdown

Fuel combustion generates the power that moves a vehicle forward. In a typical heavy truck, the engine consumes over half of the fuel in thermodynamic and friction losses. Work done against the external forces of rolling resistance, grade and aerodynamic drag is responsible for most of the remaining fuel consumption. Additional losses originate from acceleration, braking and accessories such as fan. Tractive force can also be generated by conversion of gravitational potential energy when the truck travels downhill. In general, the fuel consumption distribution varies along the route because of changes in the road grade, wind, pavement, vehicle speed and traffic. As an example, Figure 2.2 shows the TRMA-estimated fuel breakdown for the MnROAD truck loaded to 80,000 lbs. traveling on the Mainline.

Measuring fuel consumed by each dissipative force in the truck is challenging. Current methods require stringent SAE procedures [5, 6]. However, these tests may measure only a single dissipative force, such as aerodynamic drag [5] and cannot provide the entire fuel breakdown.

The procedure described in this final reports offers an alternative to current testing practices. Tests can be performed on any road in two-to-three hours with off-the-shelf equipment. The experimental setup comprises a logger for collecting engine data, weather stations for wind speed and direction, and a differential GPS unit for road elevation. TRMA then estimates the complete fuel breakdown from the instantaneous engine brake torque and fuel rates, and distributes it over all the forces acting on the truck (see Reference 4 for a complete description of the power balance equations).

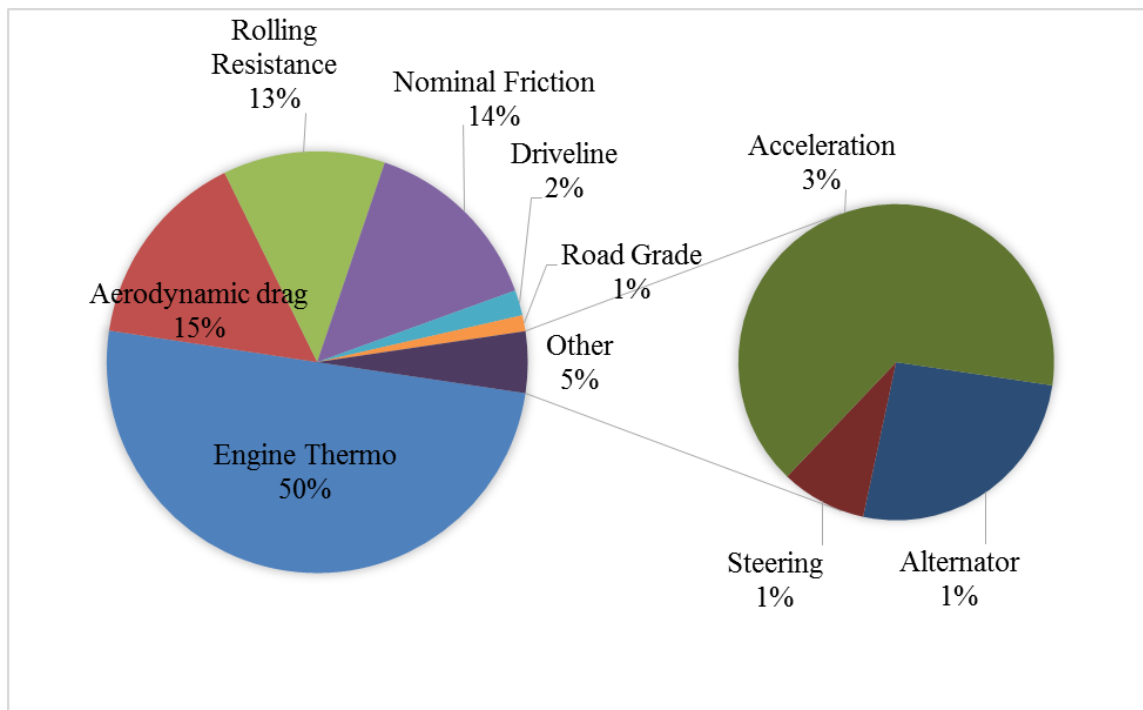


**Figure 2.2 Estimated fuel consumption breakdown of the MnROAD truck traveling on the Mainline at 64 MPH.**

## Estimation of Power Consumed by Dynamic Rolling Resistance

Rolling resistance is a non-conservative force resulting in energy dissipation. Consumed power is given by [4]:

$$P_{RR} = \dot{x}F_{RR} = \mu_{RR}\dot{x}F_z = \dot{x}\mu_{RR}[(M_w + M_c)g \text{Cos}(\chi_{road})] + \dot{x}\mu_{RR}[M_w\ddot{u}_w + M_c\ddot{u}_c] \quad (2.3)$$

or

$$P_{RR} = P_{RR,Static} + P_{RR,Dynamic} \quad (2.4)$$

Where  $P_{RR,Static}$  and  $P_{RR,Dynamic}$  are the static and dynamic contribution, respectively. The energy transferred into the vehicle vertical motion is eventually dissipated into heat by damping in the suspensions and tires. The power consumed by a damper acting on a particle moving in the z-direction is given by [7]:

$$p(t) = |\text{Force} \cdot \text{Velocity}| = d \cdot \dot{z}^2 \quad (2.5)$$

Where  $d$  is the damping coefficient and  $\dot{z}$  is the velocity of the particle under damped oscillatory motion. In QCM, there are two types of particles executing a damped motion: suspensions and tires. The velocity of the tire is that of the unsprung mass (Figure 2.1). The damped velocity of the suspension, sprung mass, is measured relative to the tire.

For stationary random processes, the average power consumed  $\bar{P}$  is equal to the mean square value of the relative velocity multiplied by the damping coefficient. It can be computed from the spectral density of the velocity [7]. It can be expressed terms of the relative acceleration,  $\ddot{z}$ , as:

$$\bar{P} = d \cdot E[\dot{z}^2] = d \int_{-\infty}^{+\infty} S_{\dot{z}}(\omega) d\omega = d \int_{-\infty}^{+\infty} \frac{1}{\omega^2} S_{\ddot{z}}(\omega) d\omega \quad (2.6)$$

In Equation 2.6,  $E$  is the expectation value,  $S_{\dot{z}}(\omega)$  and  $S_{\ddot{z}}(\omega)$  are the spectral densities of velocity, and acceleration, respectively, and  $\omega = 2\pi f$  is the angular speed.

The total power consumed by a single axle, for example front axle, consisting of two suspension dampers and two tires is [7]:

$$\bar{P} = 2 \cdot \left( d_s \int_{-\infty}^{+\infty} S_{\ddot{z},s}(\omega) / \omega^2 d\omega + d_w \int_{-\infty}^{+\infty} S_{\ddot{z},w}(\omega) / \omega^2 d\omega \right) \quad (2.7)$$

Where  $d_s$  is the effective suspension damping coefficient,  $d_w$  is the tire damping coefficient. The spectral densities of suspension,  $S_{\ddot{z},s}$  and tire,  $S_{\ddot{z},w}$  are computed from the Fourier transforms of the accelerations of sprung and unsprung masses, respectively. In a tandem axle there are two single axles and each axle has four tires. Equation 2.7 for a tandem axle becomes:

$$\bar{P} = \left( 4d_s \int_{-\infty}^{+\infty} S_{z,s}(\omega) / \omega^2 d\omega + 8d_w \int_{-\infty}^{+\infty} S_{z,w}(\omega) / \omega^2 d\omega \right) \quad (2.8)$$

### Spectral Analysis of Vibrations from Tires and Suspensions

During travel, suspensions and other components such as fuel tanks, engine and transmission, excites vibrational modes in the 1-25 Hz range [8]. Truck vibrations are typically classified into two groups: excitations of suspensions from road roughness/unevenness and excitations from “on-board” sources, such as fuel tanks and engine, driveline and tire/wheel assemblies [8]. Bounce, roll and pitch rigid motions of the chassis give rise to the lowest frequencies, while tandem bounce motion and vibrations from on-board source are observed above 5 Hz [8]. Vertical acceleration of tires/wheel assembly at high speeds results in vibrations between 30 and 100 Hz [8]. All these vibrations occur below the human audible range or are perceived as low bass tones. Audible frequencies, or “road noise”, are produced from the compression and pumping of the air between the tire threads and the pavement at high vehicle speeds. They manifest in the so called “multi-coincident” peak between 700-1,300 Hz [9]. The mechanisms of road noise generation have been examined in detail [9-11]. Coincident frequencies were not examined here because the test truck instrumentation limits analysis to below 600 Hz.

The distribution of truck vibrations over different pavement types was computed from the Power Spectral Density (PSD) obtained from the autocorrelation function of the Fourier spectra. The power dissipation by a vibrational mode drops quadratically with the increasing frequency as seen in equation 2.6. Since the lowest frequency vibrations are due to the suspensions, their dampers are expected to contribute the most to dynamical rolling resistance.

### CHAPTER 3: NUMERICAL CONSIDERATIONS

The MnROAD test truck weighs 80,000 lbs. and it experiences a rolling resistance force of about 2,400 N. The contribution of the dynamic component is expected to be about 10%, or 240 N. TRMA predicts the accuracy of estimated parameters, including CRR, in terms of the computed residual force that is the sum of all forces acting on the vehicle. Theoretically, the residual force should be zero. Since the sum of all the forces, i.e. the residual force, is zero, TRMA can compute one of the forces if all others are known. Accuracy of the TRMA was previously estimated by predicting the grade (force) and comparing the predictions to direct differential GPS measurements. Using this approach, the TRMA estimated the road grade of the Mainline within  $\pm 0.05$  degrees uncertainty, well below the observed grade variations [4]. However, due to the large mass of the truck, the grade force accuracy is still significant: 310 N. Additional uncertainties arose from engine torque output and driveline efficiencies. The uncertainty in driveline efficiency and brake torque were  $\pm 301.4$  N [4]. Therefore, the magnitude of dynamic rolling resistance is within the margin of parameter estimation error of the model. Spectral analysis is chosen here to overcome the limitation of uncertainties in quasi-static force estimation. Since dynamical rolling resistance is caused by time dependent forces above one Hz, the spectral analysis filters out all static forces and their related uncertainty.

Accelerometer data could not be incorporated directly into the TRMA because the current instrumentation setup did not allow synchronization of DGPS, accelerometers signals, and data streaming from the Controller Area Network (CAN) of the truck, such as vehicle speed, RPM and applied torque. Because of this instrumental limitation, the vibrational motions, as recorded by accelerometers, are treated as an isolated system that is constantly excited by the pavement and whose energy is dissipated by the dampers. Over sufficiently long periods of time, the energy input and the energy dissipation rates are considered equal. Therefore averaged dynamical rolling resistance can be estimated from the average energy dissipation rates.

In this final report, the dynamic contribution to rolling resistance is computed directly from the accelerometer sensor data and Eq. (2.7). Table 3.1 summarizes utilization of experimental data in estimating desired physical quantities.

**Table 3.1 Computed Physical Quantities.**

<b>Physical Quantity</b>	<b>Experimental Data</b>	<b>Modeling Approach</b>
Contact Forces	Accelerometers	Eq. (2.1)
Static Rolling Resistance	Vehicle ECU data, road grade, weather data	TRMA
Dynamic rolling resistance	Accelerometers	Eq. (2.7)
Power consumption	Accelerometers, vehicle ECU, etc.	TRMA, Eq. (2.7)
Fuel Consumption	Accelerometers, vehicle ECU, etc.	TRMA, Eq. (2.7)

## CHAPTER 4: EXPERIMENTAL SETUP

### Vehicle Instrumentation

The instrumented truck has been described previously [12]. Briefly, a WorkStar heavy duty vehicle (the “MnROAD Truck”) had accelerometers mounted on axles and frame rails and a differential GPS (Trimble R8) unit mounted on the cab’s rear. A schematic of the truck instrumentation is shown in Figure 4.1.

A compact RIO (cRIO) system from National Instruments (NI) digitized signals from accelerometers and a Trimble R8 GPS unit, and fed into a LabVIEW data logging application provided by MnROAD. Accelerometer signals were acquired at a frequency of 1,200 Hz and the R8 signals were recorded every 0.1 sec.

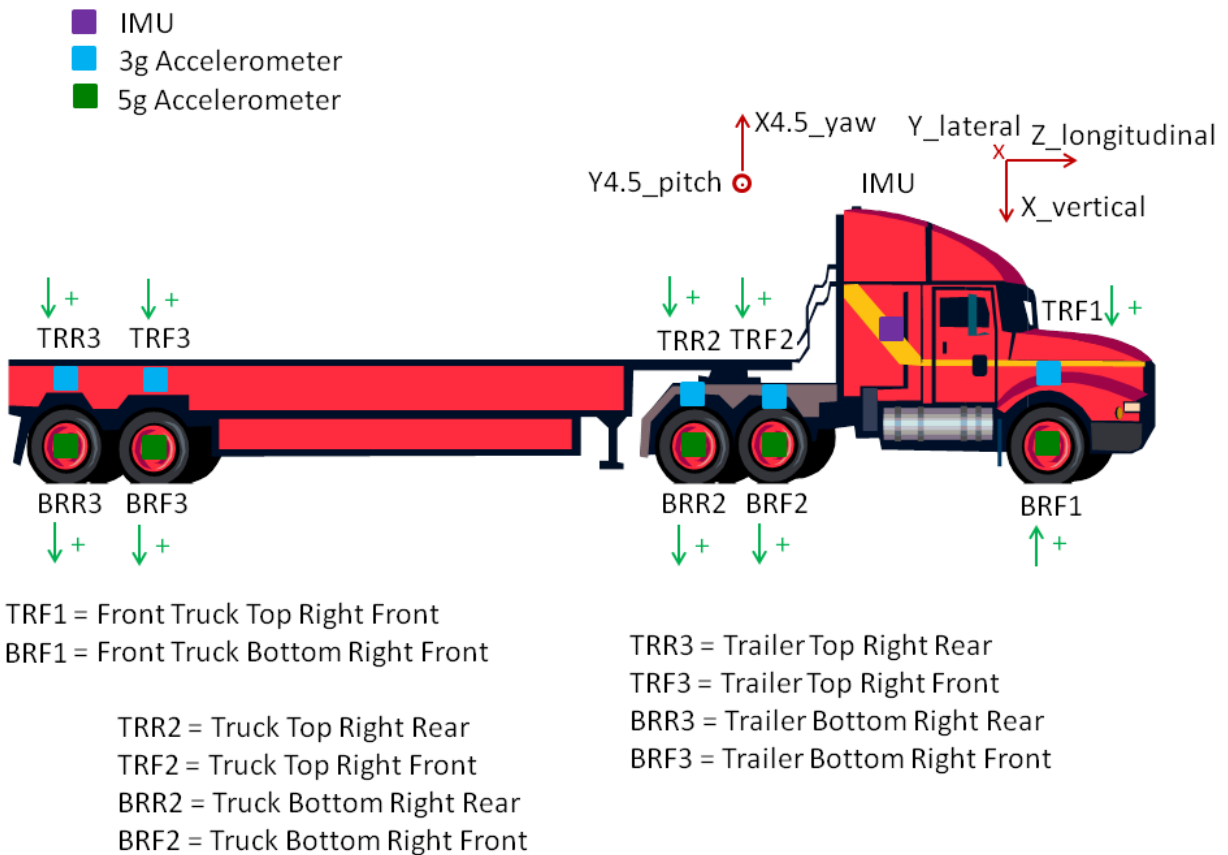


**Figure 4.1 Instrumentation of MnROAD Truck, driver side view (revised from Ref. [12]).**

A FuelMiner Logger logged, without any loss, all data streaming from the Controller Area Network bus (CAN) of the MnROAD truck. (Figure 4.2). The Logger plugs into the J1939 port in the cab and has a wireless GPS/GSM module for real time monitoring [13]. The Logger recorded data includes torque, speed, RPM, transmission gear, instant fuel consumption and

ambient temperature. Over 300 parameters are broadcasted from CAN [14] at rates up to 50 Hz. The Logger also recorded location from the GPS unit every second. All data were encrypted and stored in a flash memory card inside the unit. Over 5,000 vehicle data points were available for each Mainline test cell at 30 MPH.

Two MnROAD weather stations [15] at the North-West and South-East ends of the Mainline recorded ambient data during testing on the Mainline. These included temperature, wind speed and direction, and barometric pressure. Data were recorded every five seconds.

Two ultrasonic anemometers provided by FuelMiner recorded wind data during the tests on TH 10 and TH 66. The R.M. Young marine ultrasonic anemometers were placed by the side of road, one in each direction, and data received every second were saved into a data logger built by FuelMiner. The anemometer on TH 10 is shown in Figure 4.3. Ambient temperature was recorded as broadcasted by the vehicle CAN.



**Figure 4.2 FuelMiner Logger.**

### **Test Procedure**

Data were recorded while driving the MnROAD Truck loaded to 80,000 lbs. at different cruise speeds over the chosen road sections. The vehicle was warmed up for a minimum of 30 minutes before the start of each test. Several passes in each direction were recorded. Constant speed was maintained by driving on cruise control.

The Mainline road closure on October 20 provided ideal testing conditions. On TH 10 and TH 66, traffic somewhat limited the ability to drive on cruise control and at sustainable vehicle speeds. Several runs were completed on both highways in about two hours to insure sufficient data collection under nearly identical conditions.



**Figure 4.3 Ultrasonic anemometer near TH 10.**

### **Data Collection and Format**

The LabVIEW application controlling the NI cRIO was designed to operate in a triggering mode in which data were recorded for less than a minute at a time [12, 15]. However, for this project, it was operated in a continuous mode, with the only limitation being the size of the Technical Data Management Streaming (TDMS) data file. The software wrote in blocks of 512 MB that held about 30 minutes of accelerometer data. These files were then assembled manually to reconstruct the entire test sequence. Time stamps and GPS locations from the FuelMiner Logger were matched with those of the Trimble R8 on the MnROAD truck to verify vehicle speed, cruise control status, and to select start and end coordinates.

Accelerometer data were converted from the NI TDMS file format to MATLAB format using the utility *ConvertTDMS.m (v10)* obtained from the MATLABCentral File Exchange site.

CAN and GPS data recorded with the Logger were made available in CSV format. Each trip consisted of a set of CSV files grouped according to their PGN label, with each data column listing the corresponding SPNs. Labeling followed the J1939 standard nomenclature [14].

## CHAPTER 5: TEST PAVEMENTS

### MnROAD Mainline

The Mainline is 3.5-miles of Interstate traffic diverted from the parallel westbound I-94 between Albertville and Monticello, Minnesota [15]. It comprises 40 test cells of different pavement construction. A simplified representation of the Mainline, as of August 2014, into sections of either bituminous or concrete top layers is shown in Figure 5.1. Additionally, each concrete cell is constructed from panels of different lengths as described in Table 5.1.

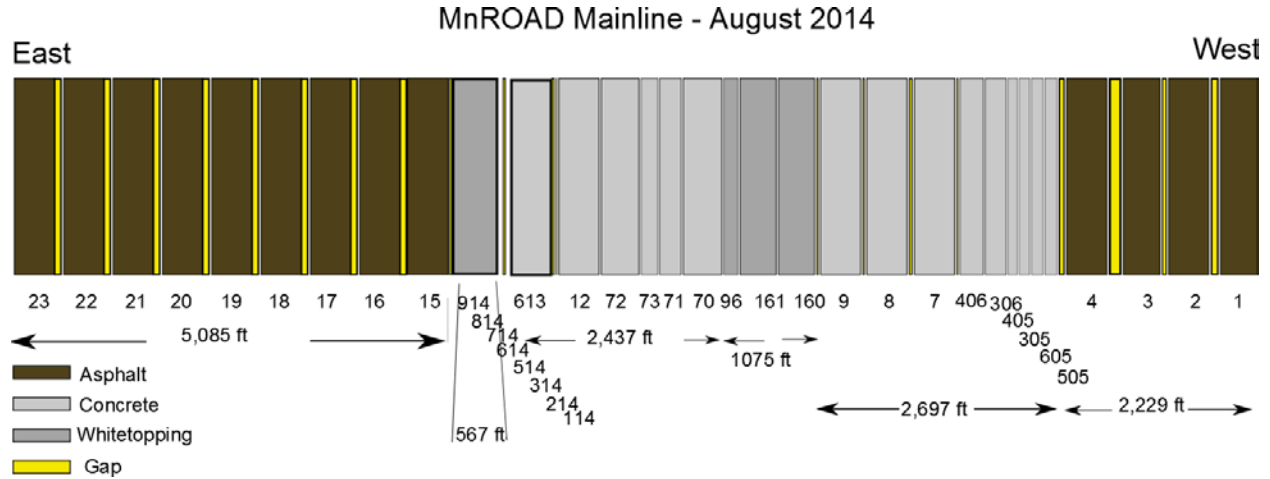


**Figure 5.1 Schematic of MnROAD pavement cells.**

**Table 5.1 Length of Mainline concrete panels**

Cell	Panel Length (feet)	Cell	Panel Length (feet)	Cell	Panel Length (feet)
914	6	613	15	9	15
814	6	12	15	8	15
714	6	72	15	7	20
614	6	73	15	406	15
514	6	71	15	306	15
414	6	70	15	405	15
314	6	96	5	305	15
214	6	162	6	605	6
114	6	160	6	505	6

## Mainline – Road Elevation and Grade

Particular attention was paid to the measurement of road elevation. Its slope determines the grade force, i.e. the force needed to move the vehicle against gravity. Accurate elevation measurements reduce the residual error in the TRMA estimates.

Two sets of elevation data from 2013 and April 2014 provided by MnROAD were used to compute the grade. It included survey data from passing, driving and centerline lanes. The slope was computed from the spherical law of cosines and by taking the average of the forward and backward direction at each measurement point. The Mainline grade used in the computations is shown in Figure 5.2

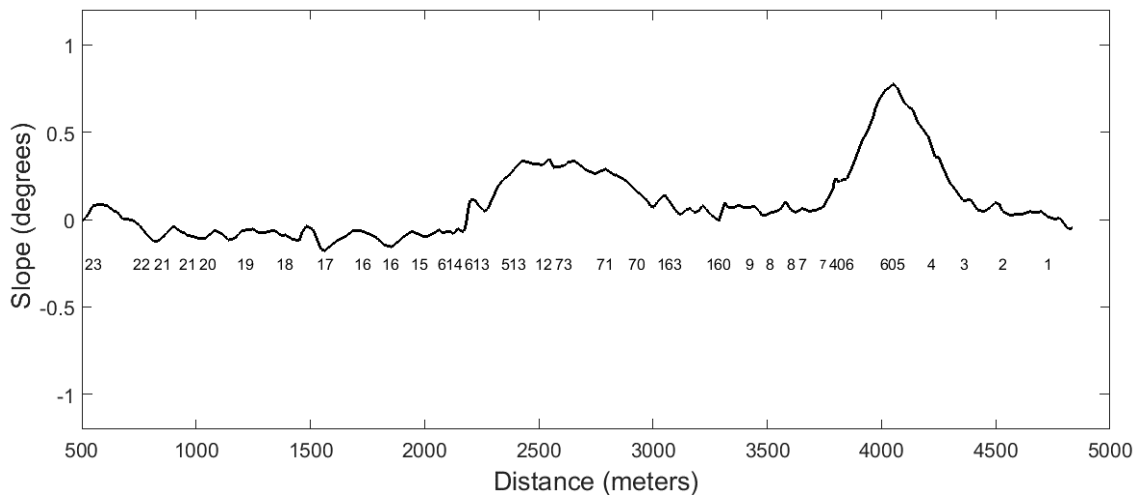


**Figure 5.2 Mainline road grade. Cell numbers are shown at the bottom of the graph.**

## Mainline – IRI

IRI was measured by MnROAD with a LISA profiler [13]. Figure 5.3 shows the IRI of the driving lane in a westbound direction. Data were collected on April 2nd, 2013.

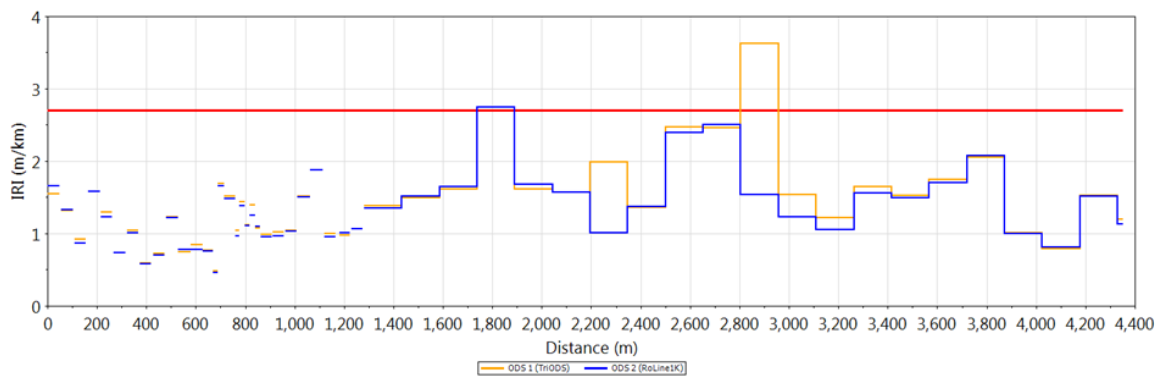


**Figure 5.3 IRI of MnROAD Mainline (westbound direction).**

## Mainline – Environmental Conditions

Data included in the analysis were collected on three days during summer and fall of 2014. Table 5.2 lists road, vehicle and ambient conditions during those measurements. Temperature varied one degree or less during the duration of each test.

**Table 5.2 Mainline environmental conditions.**

Date	Road Conditions	Start Time	End Time	Cruise Speed (MPH)	Air Temperature (Celsius)	Wind Speed (m/s)	Wind Direction (degrees)	Barometric Pressure (mBar)
10/20/14	Road Closure	9:00 am	13:00pm	30 64	14.3 ±1.4	3.8±1.0	292±109	981.0±0.3
6/12/14	Live Traffic	11:26am	13:50pm	64	14.9±0.4	4.0±1.5	290±30	976.8±0.3
6/13/14	Live Traffic	10:40am	12:10pm	64	21.4±0.3	1.5±0.8	196±52	981.3±0.6

## **TH 10 – Concrete Pavement**

The TH 10 road segment near Sartell, MN, is a divided two-lane highway. The pavement is reinforced concrete with 28 foot joint spacing. The selected segment was five miles in length and located between RP 170.5 and RP 175.5. It was constructed in 1971. The GPS coordinates of the section are listed in Table 5.3 and its map is shown in Figure 5.4.

### Road Elevation and Grade

Road elevation was measured with the Trimble R8 unit mounted in the rear of the truck's cab [12]. In addition, MnROAD measured elevation with the Ames lightweight profiler and provided District 3 (D3) survey data (courtesy of David Van Deusen). Comparison between survey, Ames and R8 elevation (Figure 5.5) showed a constant offset, but nearly identical profiles. The truck GPS data from multiple passes were combined to obtain the average grade. The resulting grade profile is shown in Figure 5.6. Direction of travel was from west to east.

### TH 10 – IRI

IRI was measured by MnROAD with the Ames lightweight profiler in the eastbound direction. The overall IRI was 2.55 m/km and it was well above the acceptable level of 2.7 m/km in numerous sections (Figure 5.7).

**Table 5.3 TH 10-GPS Coordinates.**

TH 10 (Sartell)	Latitude	Longitude
Start	45.64752	-94.17617
End	45.60345	-94.15222

TH 10 – Environmental Conditions

Data were collected on June 20, 2014. Table 5.4 lists road, vehicle and ambient conditions during those measurements that were included in the data analysis.

**Table 5.4 TH 10 Environmental conditions.**

Date	Conditions	Start Time	End Time	Cruise Speed (MPH)	Air Temperature (Celsius)	Wind Speed (m/s)	Wind Direction (degrees)
6/20/2014	Live Traffic	10:20am	13:20pm	54	31.1 ± 2.6	1.4±0.9	172±71
				65			

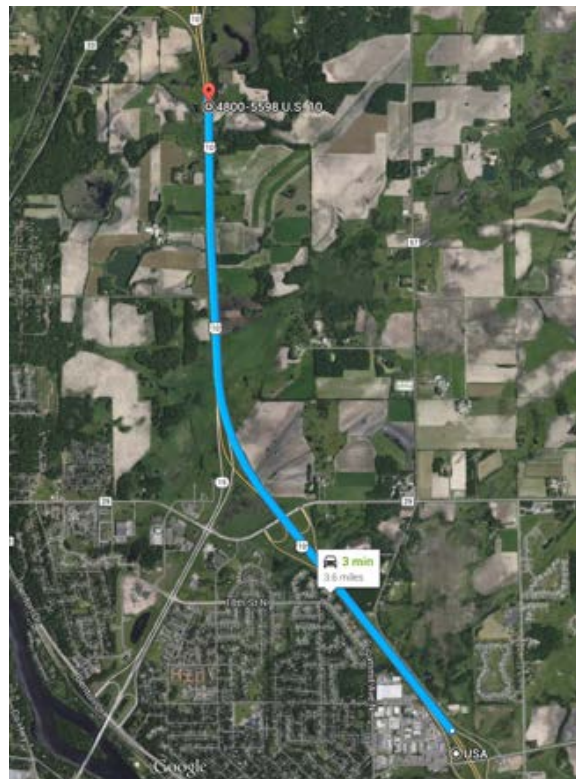


**Figure 5.4 TH 10 – Concrete pavement road section.**

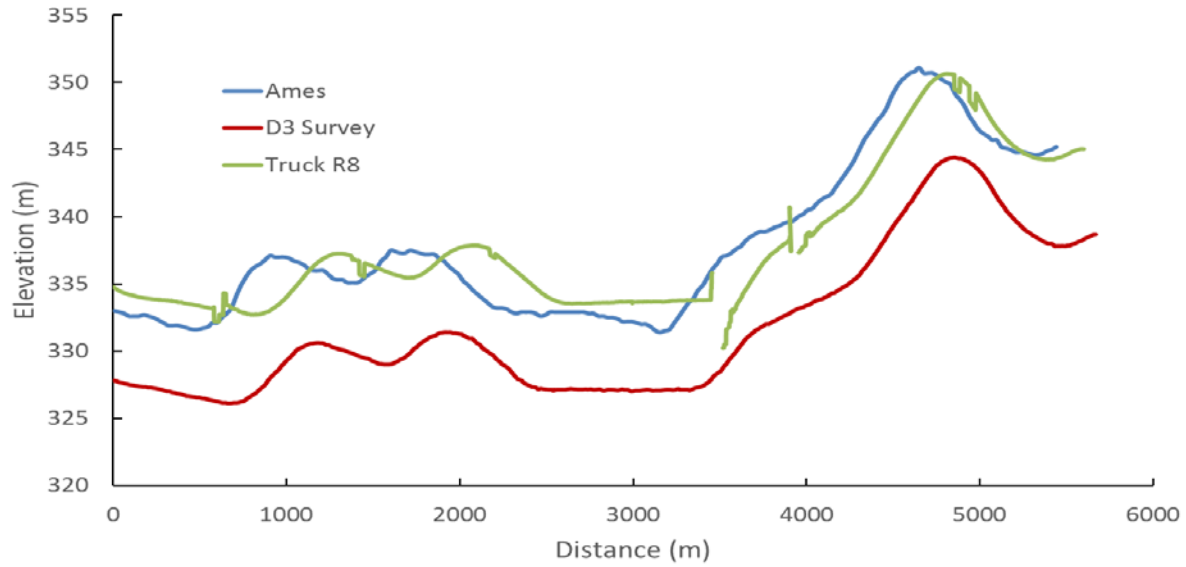


**Figure 5.5 TH 10 – Elevation.**

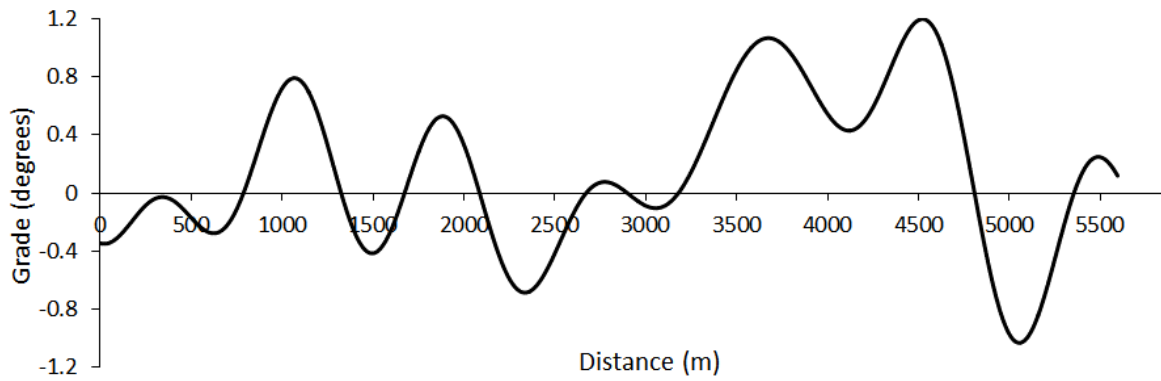


**Figure 5.6 TH 10 – Road grade.**

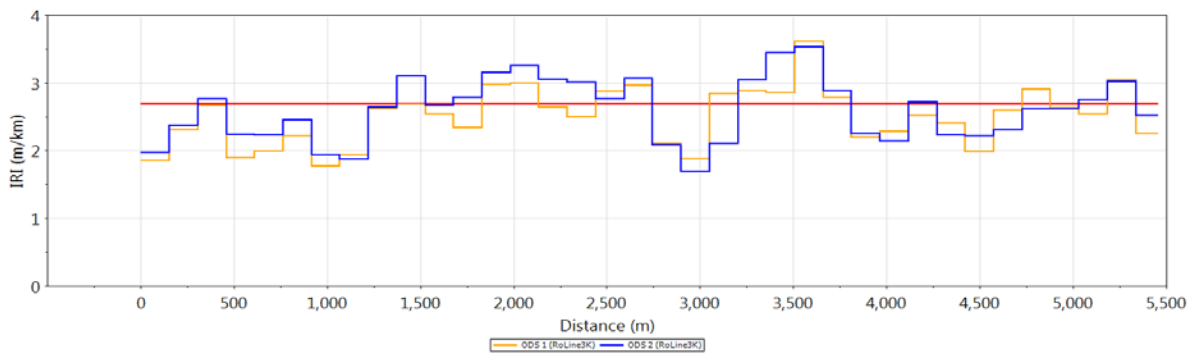


**Figure 5.7 TH 10 – IRI.**

## TH 66 – Bituminous Pavement

The TH 66 road segment immediately north of Good Thunder, MN, is a single lane roadway. The truck traveled for two miles in both directions (Figure 5.8). One ultrasonic anemometer was placed approximately halfway along the road segment. The GPS coordinates of the sections are shown in Table 5.5.

**Table 5.5 TH 66 – GPS Coordinates.**

TH 66 (Good Thunder)	Latitude	Longitude
Start	44.05739	-94.04870
End	44.03412	-94.04837

## TH 66 – Road Elevation and Grade

Road elevation was measured by MnROAD using the Ames profiler. Elevation data from the truck R8 were not recorded because the unit malfunctioned during the test. The resulting smoothed grade curve obtained from the profiler data is shown in Figure 5.9. Direction of travel is from south to north.

## TH 66 – IRI

IRI was measured by MnROAD using the Ames lightweight profiler. The overall IRI was 2.65 m/km but well above the acceptable level of 2.7 m/km in numerous sections (Figure 5.10Figure 5.3).

## TH 66 – Environmental Conditions

Data were collected on June 23, 2014. Table 5.6 lists road, vehicle and ambient conditions during those measurements included in the data analysis.

**Table 5.6 TH 66 – Environmental conditions.**

Date	Conditions	Start Time	End Time	Cruise Speed (MPH)	Air Temperature (Celsius)	Wind Speed (m/s)	Wind Direction (degrees)
6/23/2014	Live Traffic	11:20AM	13:00PM	45	31.9 ±1.6	3.2±0.9	318±63
				54			



**Figure 5.8 TH 66 – Bituminous pavement road section.**

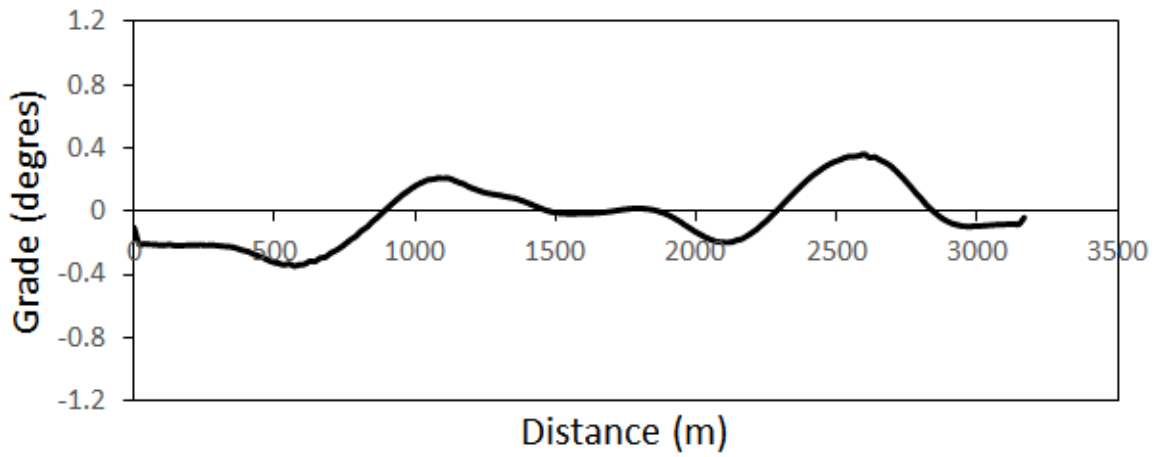


**Figure 5.9 TH 66 Road grade**

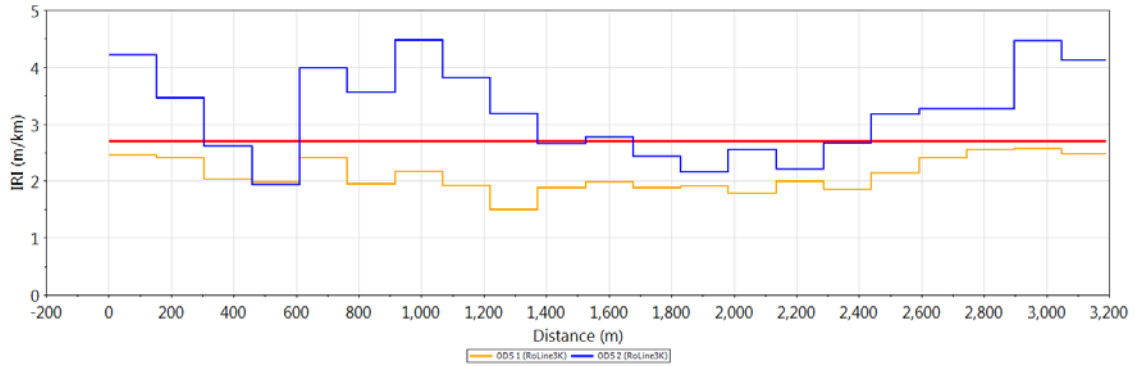


**Figure 5.10 TH 66 – IRI.**

# CHAPTER 6: DATA ANALYSIS

## Contact Forces

Ground contact forces acting on the tires were computed from Eq. (2.1). The total, sprung and unsprung masses of the MnROAD truck are listed in Table 6.1. The masses of the individual vehicle components are given in Table 6.2. The grade angle was set to be  $\chi_{road} = 0$  because the Mainline grade is less than 1 degree (Figure 5.2). Contact forces for representative runs on the Mainline at 30 and 64 MPH are shown in Figure 6.1. The dynamic components from Eq. (2.1) amount to 5-10% of total contact forces.

**Table 6.1 Total, sprung and unsprung mass of MnROAD truck.**

Definition	Notation	Mass (kg)
Total Mass = front axle + rear axle + trailer axle loads	$M_c + M_w$	36,152
Unsprung Mass = tires + wheels	$M_w$	1,463
Sprung Mass = Total Mass - Unsprung Mass	$M_c$	34,689

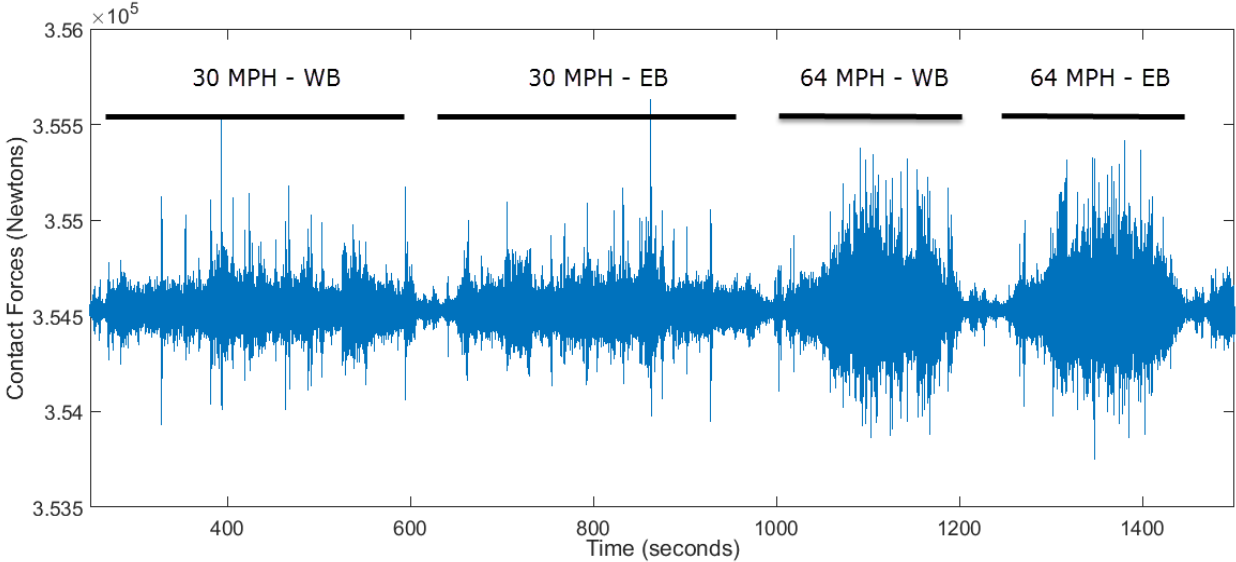


**Figure 6.1 Mainline – Contact forces.**

**Table 6.2 Vehicle mass**

<b>VIN</b>	<b>1HSGSSJT8CJ536729</b>
Front Axle Load	5,307 kg
Drive Axle Load	15,468 kg
Trailer Axle Load	15,377 kg
Front/Rear Wheel Mass	20 kg
Rear Tire (XDN2 Michelin 275/80R22.5) Mass	60 kg
Front Tire (315/80R22.5 HS U Continental) Mass	69 kg
Front Axle (Meritor MFS-16-143A) Mass	193 kg
Rear Axle (Meritor RT-40-145) Mass	255 kg
Front Suspension (Spring Parabolic)Mass	100 kg
Rear Suspension (Hendrickson PRIMAAX EX) Mass	506 kg

### **Rolling Resistance and Fuel Consumption**

#### Coefficient of Rolling Resistance of Mainline Cells

The rolling resistance force was computed from Eq. 2.2. The road grade (Figure 5.2) was assumed a known parameter and rolling resistance force was computed from the force balance, as described in Chapter 3. Data from the test on October 20, 2014 were used in the analysis. The vehicle speed was 30 MPH. The result of the TRMA is shown in Figure 6.2. The Coefficient of Rolling Resistance Coefficient (CRR) varies between 0.0044 (Cell 4) to 0.0072 (Cell 306), with an average value of 0.0055 (Table 6.3). The range of CRR values and trends is qualitatively similar to that reported by Ejsmont and Ronowski for car tires [16].

The CRR was also obtained for the vehicle driving in live traffic conditions at 64 MPH (Figure 6.2). The average CRR is 0.0059 $\pm$  0.001 for June 12 and 0.0070  $\pm$  0.001 for June 13. The discrepancy in CRR between the two runs may be due to different environmental conditions (see Table 5.2).

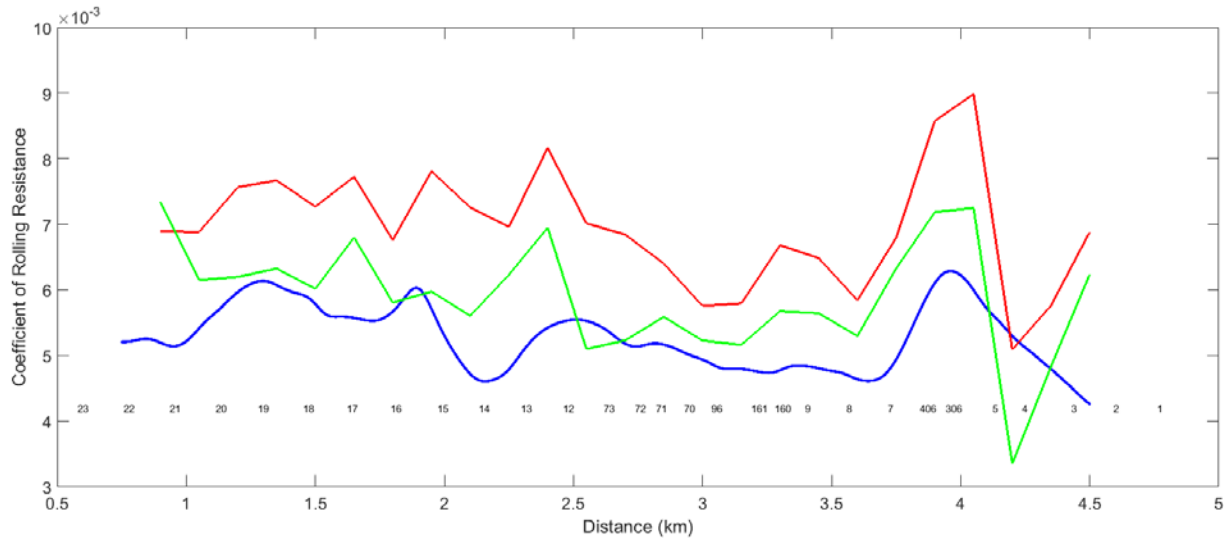


**Figure 6.2 Coefficient of rolling resistance computed from data recorded at 30 MPH and at 64 MPH. Blue: 30 MPH; red: June 12; green: June 13.**

Rolling Resistance of TH 10 and TH 66

The rolling resistance was estimated for the two highway sections using the TMRA model. The results are shown in Table 6.4. The computed CRR was 0.0061 for the TH 66 bituminous pavement and 0.0072 for the more rigid TH 10 concrete pavement.

**Table 6.3 CRR of Mainline Cells (30 MPH)**

Cell Number	CRR	Location*
23	0.0061	0.5793
22	0.0048	0.7567
21	0.0049	0.9341
20	0.0054	1.1139
19	0.0061	1.2782
18	0.0061	1.4530
17	0.0063	1.6225
16	0.0055	1.7925
15	0.0056	1.9737
14	0.0055	2.1346
13	0.0060	2.2978
12	0.0059	2.4599
73	0.0058	2.6163
72	0.0055	2.7382
71	0.0054	2.8193
70	0.0051	2.9283
96	0.0052	3.0331
161	0.0053	3.1900
160	0.0052	3.2793
9	0.0056	3.3972
8	0.0055	3.5561
7	0.0052	3.7166
406	0.0065	3.8419
306	0.0072	3.9409
5	0.0051	4.1224
4	0.0044	4.2374
3	0.0047	4.4270
2	0.0055	4.5915
1	0.0060	4.7625

\*distance (km) computed from GPS location (45.249694,-93.686217)

**Table 6.4 CRR of TH 10 and TH 66.**

Road	Rolling Resistance	Covariance
TH 10	0.0061	1.89 E-4
TH 66	0.0072	1.09E-4

## Fuel Consumption of Mainline Cells

The breakdown of fuel consumed by individual dissipative components was estimated by TRMA. Figure 6.3 shows the fuel consumed by rolling resistance of the truck over individual cells and driven at 30 MPH. As expected, the trend follows that of the CRR in Figure 6.2. Fuel consumed by rolling resistance at 30 MPH varied between 0.006 liter and 0.009 liter per cell (of 500 foot length), for an average consumption of 5 liter/100 km.

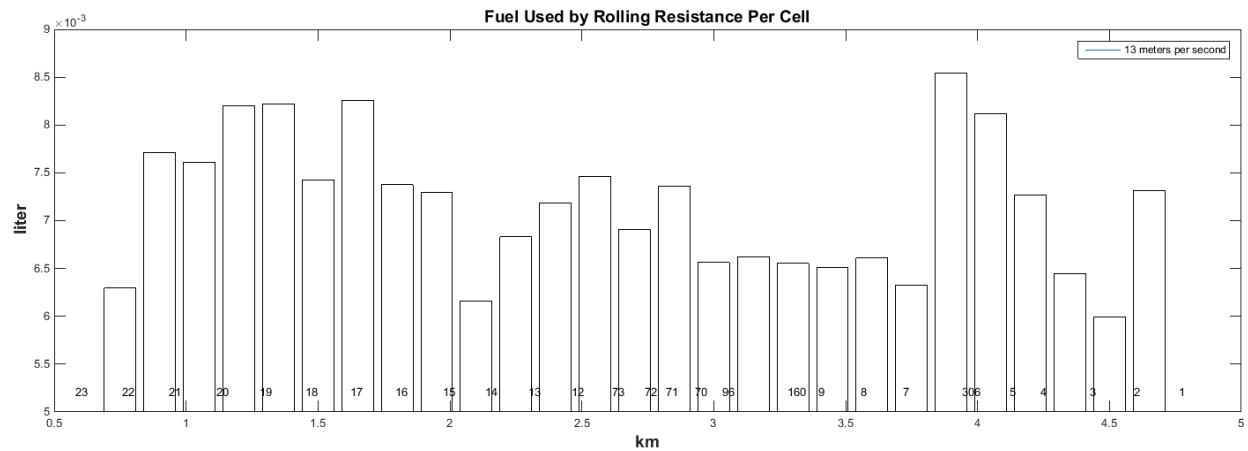


**Figure 6.3 Fuel consumed by Rolling Resistance per cell.**

## Estimated Fuel Consumption Breakdown

Fuel breakdown was estimated with TRMA [4] and it is shown in Figure 6.4. Fuel losses from the engine and nominal friction was greater at 30 MPH (71%) than at 54 MPH (65%) because the MnROAD truck engine is less efficient at low speed and frictional losses are higher at low gearing. Aerodynamic drag contribution to fuel consumption increased fourfold because of its cubic dependence on vehicle speed. Percentage wise, rolling resistance contributed slightly more at higher speeds. The remaining fuel consumption was due to acceleration and accessories. Even though the truck was in cruise control, some acceleration was needed to maintain constant speed. Accessories losses included engine fan, alternator and steering.

The computed fuel breakdown for TH 10 and TH 66 have similar profiles and the aero contribution is indicative of the 55 MPH speed (Figure 6.5).

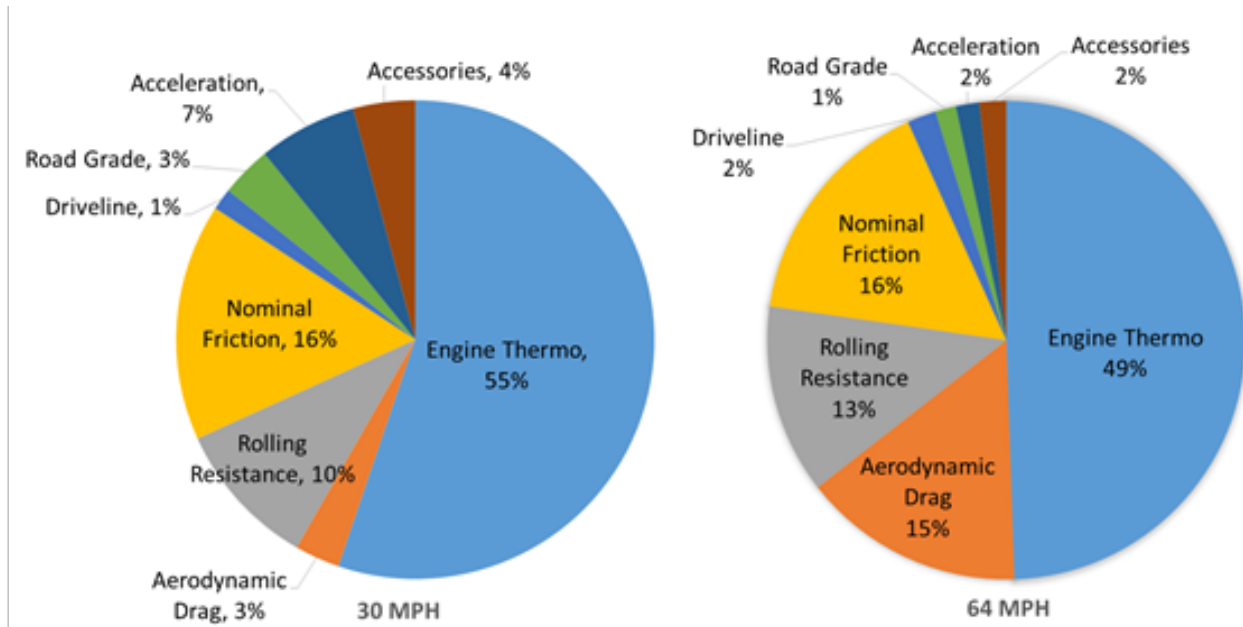


**Figure 6.4 Estimated fuel breakdown at 30 MPH and 64 MPH on the Mainline**

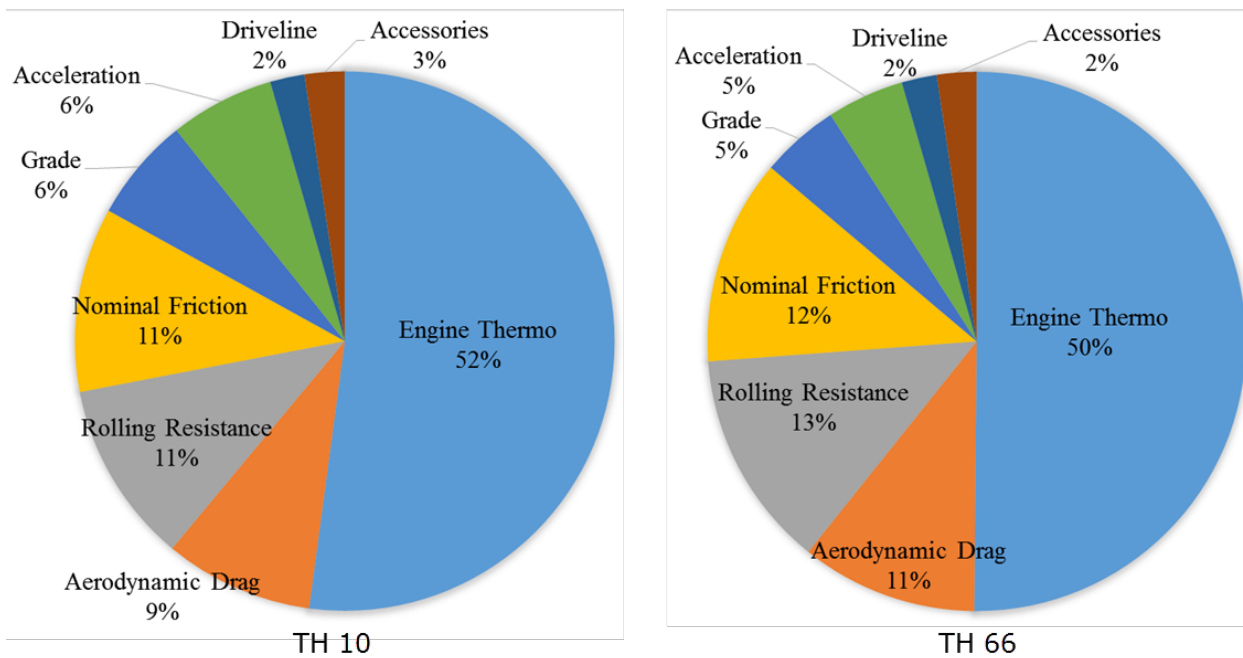


**Figure 6.5 Estimated fuel breakdown at 55 MPH on TH 10 and TH 66.**

## Spectral Analysis and Power Loss from Suspensions and Tires

### Mainline

#### *Spectral Frequencies*

The power spectral density (PSD) of truck vibrations traveling on the Mainline at 30 MPH is shown in Figures 6.6-6.8 for accelerometers TLF2, TLR2 and TLF1, respectively. Each spectrum is the PSD computed over a section roughly the length of one cell, or 500 feet. The direction of travel was from east to west.

Frequency modes below 4 Hz were associated with rigid body translational and vertical motions [8]. Bounce and pitch motions occurred between 4-5 Hz. The tandem axle contributed to modes between 7-13 Hz, as observed in the PSD of TLR2 and TLF2, but not TLF1. The mode at 16.81 Hz was assigned to the tractor tandem roll motion [8]. Of notice, the 2.904 Hz frequency mode was only observed for the concrete sections.

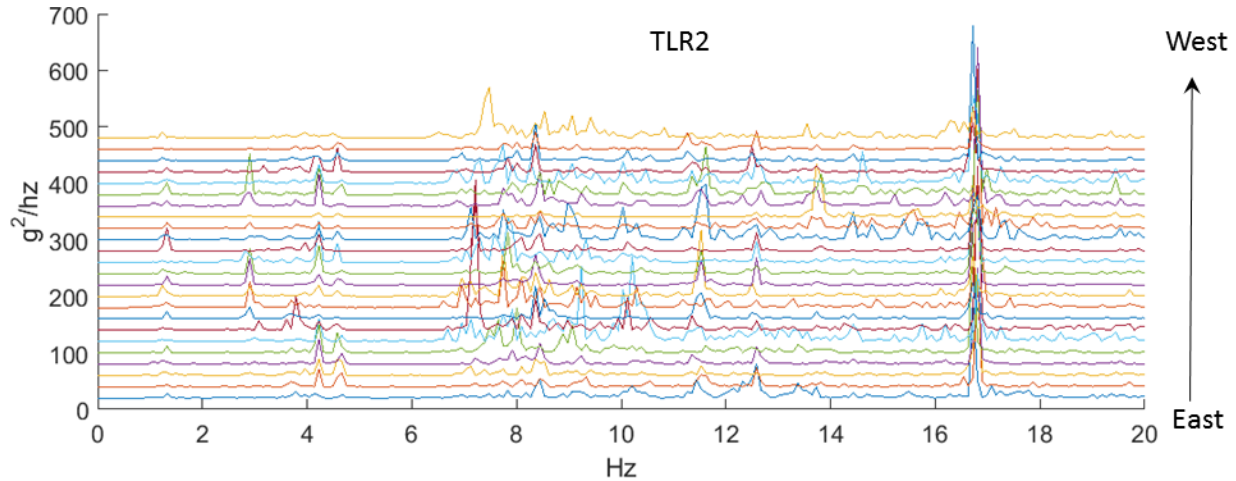


**Figure 6.6 Vibrational modes computed from accelerometer TLR2 on the Mainline.**

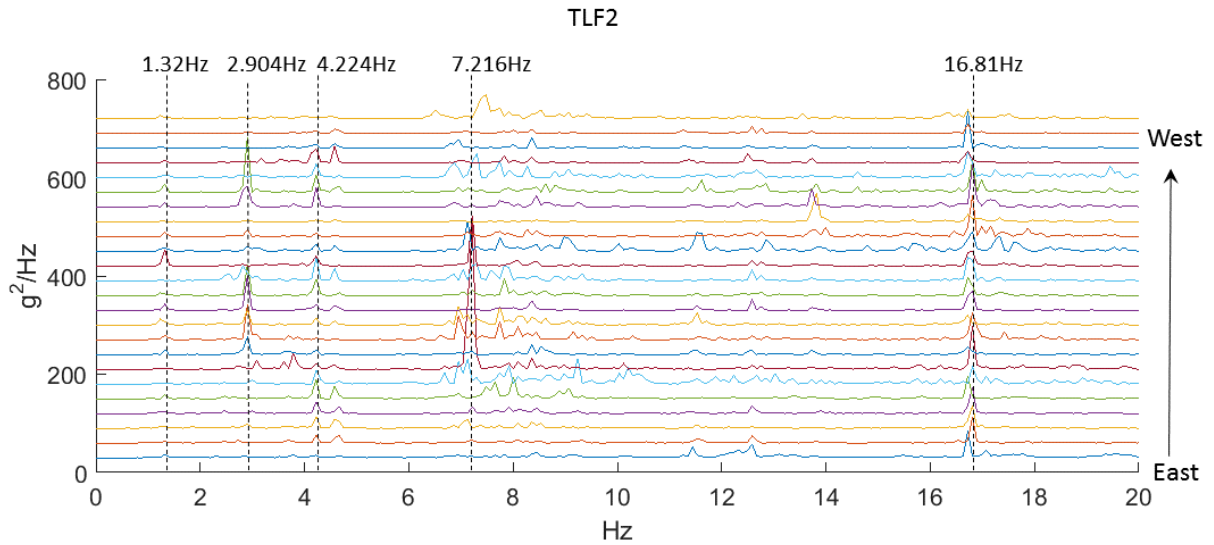


**Figure 6.7 Vibrational modes computed from accelerometer TLF2 on the Mainline.**

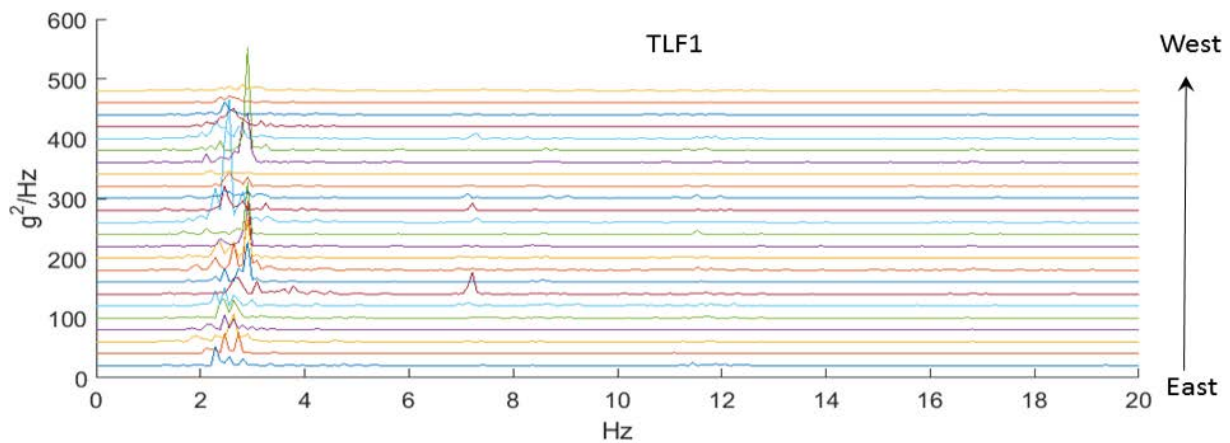


**Figure 6.8 Vibrational modes computed from accelerometer TLF1 on the Mainline.**

*Computed power loss of suspensions*

Power loss from suspensions and tires was computed from Eq. (2.7). A damping constant of 20,000 Ns/m per axle for suspensions and 4,000 Ns/m per tire was chosen based on values reported in the literature [17].

The results are shown in Figure 6.9 for vehicle speed of 30 MPH for eastbound and westbound directions. Each data point was the sum over non-overlapping 500 foot long segments, or approximately the length of one cell. Cell 20 was chosen as the reference starting point. The eastbound and westbound data were for the most part reproducible. Power loss for the MnROAD concrete and asphalt sections ranged from 250 to 1,294 watts and 211 to 1,124 watts, respectively. The average and standard deviation of power loss for MnROAD concrete sections

was 652 and 259 watts, respectively. For the bituminous sections it was 442 and 227 watts (see Table 6.5).

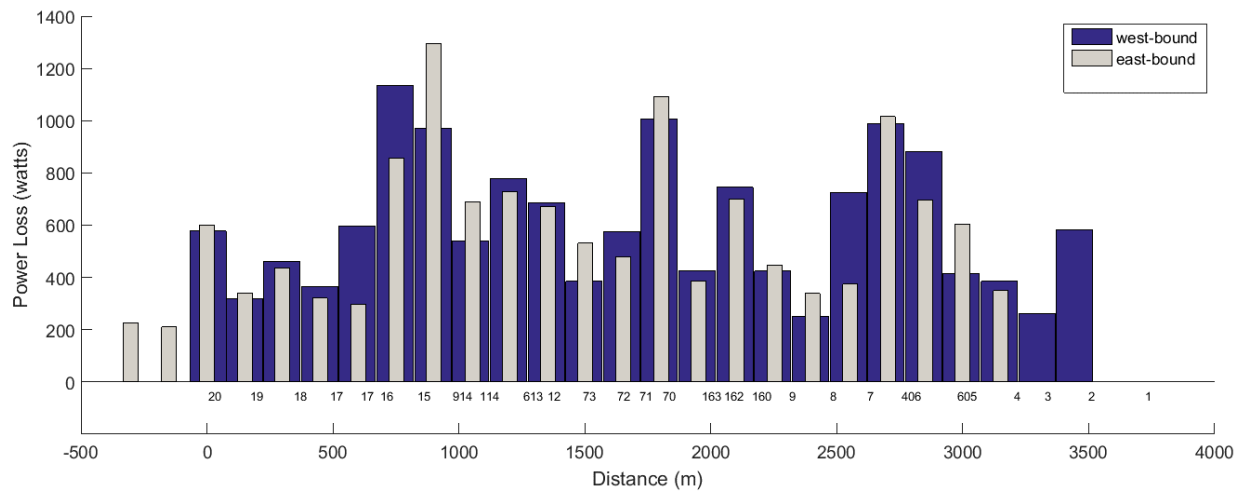


**Figure 6.9 Power loss at 30MPH for eastbound and westbound directions on Mainline.**

**Table 6.5 Average power loss of bituminous and concrete sections of Mainline.**

Section	Average Power Loss (Watts)	Standard Deviation (Watts)	Maximum (Watts)	Minimum (Watts)
Bituminous	442	227	1,134	211
Concrete	652	259	1,294	250
Conc. – Bituminous	210		213	40

TH 10 and TH 66

*Spectral Frequencies*

The PSD of TH 10 and TH 66 are shown in Figure 6.10 and Figure 6.11. Suspensions on TH 10 had stronger spectral densities and unique vibrational modes compared to TH 66. The vibrational modes at 2.92 Hz, 5.83 Hz and 17.47 were not present in the PSD of TH 66. The 11-14 Hz frequency range shows several features in the PSD of TH 66, but distinct modes centered at 11.72 Hz are observed in the PSD of TH 10. Of notice, the mode at 2.9 Hz was also observed for the Mainline concrete sections (Figure 6.7). The comparison suggests excitation of some rigid body vibrations by only the more rigid pavements. Alternatively, they may originate from the truck being excited by the joints between concrete panels. At 30 MPH, or 13.4 m/s, the frequency at 2.9 Hz of the Mainline PSD (Figure 6.7) corresponds to a characteristic length of 4.6 m or 15 feet. This is also the length of the concrete panels of cells 73 through 70 and 406 through 305 (Table 5.1). On TH 10, with the truck traveling at 55 MPH, the characteristic length

is 27 feet, close to the 28 foot length of the concrete panels. The results suggest that joints are responsible for the 2.9 Hz mode on both Mainline and TH 10.

*Computed power loss from suspensions*

Tests at 55 MPH were included in the analysis of both highway sections. Table 6.6 reports the average power loss computed from two runs each, traveling eastbound for TH 10, and north-bound for TH 66. The power loss observed on TH 10 was greater than that on TH 66. The main reason was the presence of low-frequency modes on concrete but not asphalt (Figures 6.10-11). Because of the  $1/\omega^2$  relationship between power and frequencies (Eq. (2.6), these modes have a larger contribution than the higher frequency modes.

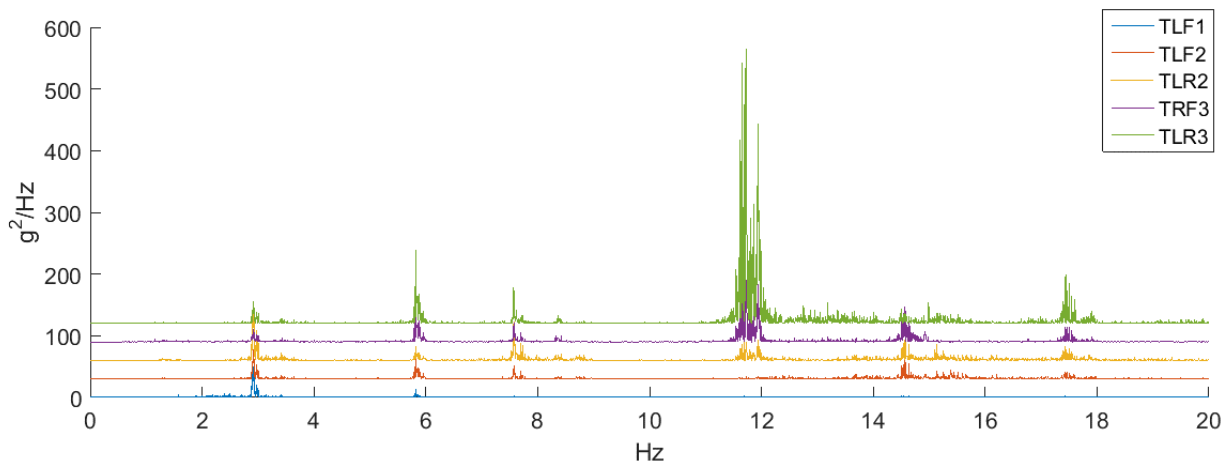


**Figure 6.10** Vibrational modes observed on TH 10. Spectra are overlaid with a shift of 30  $g^2/Hz$ .

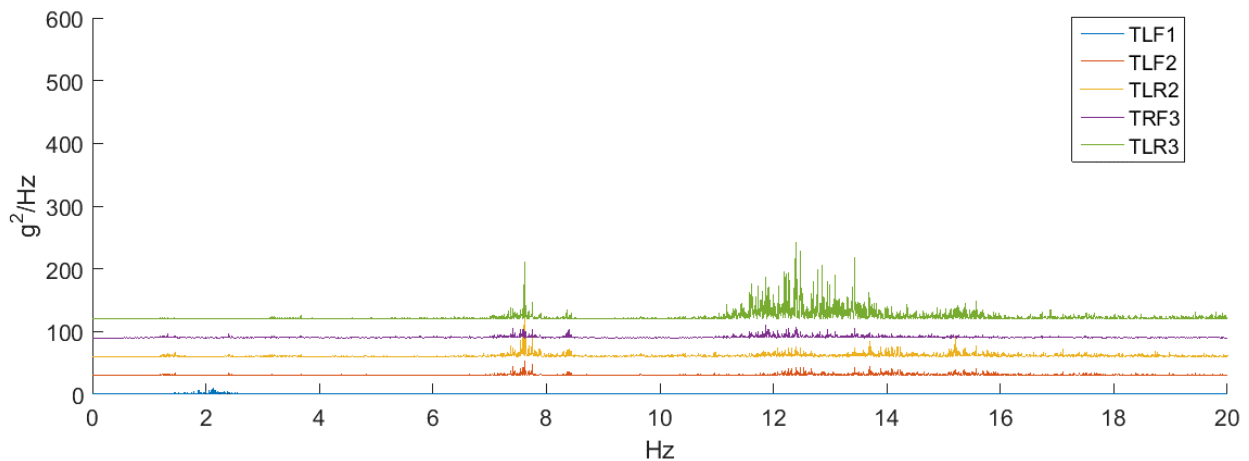


**Figure 6.11** Vibrational modes observed on TH 66. Spectra are overlaid with a shift of 30  $g^2/Hz$ .

### Contributions of Suspensions and Tires to Annual Fuel Consumption

A typical highway truck travels 120,000 miles per year with an average fuel economy of 6 MPG, for a total of 2,207 hours of operation. From Table 6.6, annual fuel consumed by suspensions and tires vibrations was 2% of total fuel for a truck driving on TH 66 and 3% for a truck driving on TH 10. The computed dynamical rolling resistance component estimates an excess of 0.3 liter/100 km, or 165 gallons of diesel per year consumed by driving over TH 10 compared to TH 66. When static contribution is included, the net fuel consumption from rolling resistance is lower for TH 10 than TH 66 because of its smaller CRR (Table 6.4).

**Table 6.6 Power loss from tires and suspensions on TH 66 and TH 10**

Highway	Power Loss (Watts)	Standard deviation (watts)	Hours/year	Total energy (MJ/year)	Total diesel (liter/year)	Liter/100km
Bituminous – TH 66	6,486	109	2,207	51,530	1,416	0.7
Concrete – TH 10	9,353	45	2,207	74,308	2,041	1.1
Concrete - Bituminous	2,867			22,778	626	0.3

## CHAPTER 7: CONCLUSIONS

The goal of this project was to compute rolling resistance and its contribution to fuel consumption. The coefficient of rolling resistance, contact forces and fuel consumed by rolling resistance were computed for each cell of the MnROAD Mainline and two highway segments of TH 10 and TH 66. Analysis included a fuel consumption breakdown into each resistive, tractive and dissipative components for each of the pavements tested. Rolling resistance was estimated to be 10-13% of total fuel burned by the MnROAD truck on these roads.

The contribution of dynamic rolling resistance was computed directly from the power spectra of accelerometers mounted on axles and suspensions of the heavy-duty truck. The spectral analysis showed low frequency modes unique to concrete and bituminous pavements. The fuel consumption component from dynamic rolling resistance was greater for TH 10 compared to bituminous TH 66. The results suggest that excitation of truck suspensions by the joints between concrete panels may be responsible. In a wider context, dynamic rolling resistance contributes 10% or less to rolling resistance, or 1-5% of total fuel usage. Static rolling resistance, aerodynamic drag, and engine efficiency will have a higher impact on fuel consumption of highway trucks.

The results presented in this report demonstrated the strength of the novel methodology and suggested directions for improvement.

### Strengths

- The experimental setup is simple and fast. Only a pluggable logger is necessary for the entire CAN recording. Two hours of testing at different cruise speeds over short road segments record sufficient data for analysis by TRMA. Environmental conditions during this time frame are stable, as shown in Table 5.2, Table 5.4, and Table 5.6.
- Tests can be performed under live traffic conditions, with the additional aid of a portable field anemometer for wind data. Elevation measurements from the Trimble R8 unit mounted on the truck are sufficient for computing the road grade precisely, as illustrated by the elevation data on TH 10 (Figure 5.5).
- TRMA is capable of resolving rolling resistance and associated fuel consumed for each Mainline cell (Figure 6.2).
- Spectral analysis of accelerometers signals is an effective method of “fingerprinting” different pavement types. Investigation of vibrational modes as a function of pavement type is pertinent to both the driver’s comfort and vehicle’s structural wear.
- Fuel consumed by dynamic rolling resistance can be computed directly from the accelerometer data and for each pavement type.

### Improvements

- The experimental setup could benefit from synchronization between the data streaming from the vehicle’s CAN, accelerometers, and differential GPS unit. Synchronization was attempted with the FuelMiner SensorNet apparatus, consisting of a wireless network of accelerometers communicating with a secondary channel of the Logger device. However,

synchronization did not fully succeed because of the limitations in the transmission rate of large data packets and the electrometric shielding of the signals by the frame rails of the truck.

- Synchronized accelerometer data could be added to the TRMA model to improve the accuracy of the measurements. With this data, QCM model, and accounting of the coupling to the longitudinal motion, it would reduce the uncertainty in the rolling resistance to less than 200 N (Chapter 3).
- Synchronized data would more accurately identify the start and end point of each Mainline cell and improve spectral characterization.
- Inclusion of turbulence effects in the computation of aerodynamic forces may increase the accuracy of the TRMA model, and indirectly, the estimation of rolling resistance for trucks traveling at high speeds. Yucel et al. has recently proposed a method for recording turbulence data [18].

## REFERENCES

- [1] Table 4-5. Fuel consumption by mode of transportation in physical units. Bureau of transportation statistics, United States Department of Transportation. Internet: [http://www.rita.dot.gov/bts/sites/rita.dot.gov/bts/files/publications/national\\_transportation\\_statistics/html/table\\_04\\_05.html](http://www.rita.dot.gov/bts/sites/rita.dot.gov/bts/files/publications/national_transportation_statistics/html/table_04_05.html). Accessed July 6, 2015.
- [2] W. F. Torrey, D. Murray. *An analysis of operational costs of trucking: a 2014 Update*. American Transportation Research Institute. Internet: [www.atri-online.org](http://www.atri-online.org). Accessed July 6, 2015.
- [3] K.Chatti, I. Zaabar (2012). *Estimating the effects of pavement condition on vehicle operating costs*. Transportation Research Board NCHRP Report 720, Washington D.C.
- [4] S. Yucel, M. Moran-Lucking, J. Magnuson, G. Paterlini, B. Worel. (2014). “Time-resolved estimation of fuel consumption breakdown of a heavy duty truck under actual road conditions”. *SAE Int. J. Commer. Veh.* 7(2):753-765, 2014, doi: 10.4271/2014-01-9030.
- [5] Society of Automotive Engineers. (2012). SAE Standard J1321. “Fuel Consumption Test Procedure - Type II”. Internet: [http://standards.sae.org/j1321\\_201202/](http://standards.sae.org/j1321_201202/). Accessed July 6, 2015.
- [6] Society of Automotive Engineers SAE. (2011). Standard J2978. “Road Load Measurement Using Coastdown Techniques”. Internet: <http://standards.sae.org/wip/j2978/>. Accessed July 6, 2015.
- [7] T.-T. Fu, D. Cebon (2003). “Economic evaluation and the design of vehicle suspensions”. *Int. J. Veh. Des.* 125-161.
- [8] T. D. Gillespie (1985). “Heavy truck ride”. SAE Technical Paper 850001, doi:10.4271/850001. Internet: <http://papers.sae.org/850001/>. Accessed July 6, 2015.
- [9] U. Sandberg (2003). “The Multi-Coincidence Peak around 1000 Hz in Tyre/Road Noise Spectra”. Paper ID 498. 5th European Conference on Noise Control. Euronoise 2003. May 19-23 2003, Naples, Italy.
- [10] B. I. Izevbekhai, (2012). “Tire pavement interaction noise of concrete pavements”. Ph.D. Thesis Dissertation. University of Minnesota, Minneapolis, MN.
- [11] R. Bernhard, R. L. Wayson “An Introduction to Tire-Pavement Noise of Asphalt Pavement”. Internet: <http://www.asphaltroads.org/assets/control/content/files/anintroductiontotire-pavementnoiseofasphaltpavement.pdf>. Accessed July 6, 2015.
- [12] L. Alexander, G. Phanomchoeng, R. Rajamani (2013). *Instrumentation of Navistar Truck for Data Collection*. MnDOT Report #MN/RC 2013-01, MnDOT, St. Paul, MN.
- [13] FuelMiner Inc. Internet: [www.fuelminer.com](http://www.fuelminer.com). Accessed July 6, 2015.

[14] Society of Automotive Engineers SAE J1939 Standard collection. Internet: [store.sae.org/j1939/contents/](http://store.sae.org/j1939/contents/). Accessed July 6, 2015.

[15] MnROAD Research. Minnesota Department of Transportation. Internet: [www.dot.state.mn.us/mnroad/](http://www.dot.state.mn.us/mnroad/). Accessed July 6, 2015.

[16] J. A. Ejsmont, G. Ronowski, J. Wilde (2012). *Rolling resistance measurements at the MnROAD facility*. Minnesota Department of Transportation Interim Report 2012-07, MnDOT, St. Paul, MN.

[17] D. Cebon (1999). *Handbook of Vehicle-Road Interaction*. Taylor and Francis: London.

[18] S. Yucel, G. Paterlini, J. Magnuson, M. Moran-Lucking, B. Worel (2014) “A novel method for fast and cost-effective aerodynamic testing”. Oral Presentation. 2014 SAE Commercial Vehicle Engineering Congress. Rosemont IL, October 7-9, 2014.